Available online at www.sciencedirect.com

SciVerse ScienceDirect

Ceramics International 39 (2013) S747–S751

CERAMICS INTERNATIONAL

www.elsevier.com/locate/ceramint

Electrical properties of $[Ag_{0.2}(K_{0.52}Na_{0.48})_{0.8}](Nb_{1-x}Ta_x)O_3$ ceramics

Young Jun Eoh[a], Jeong Ho Cho[b], Byung Ik Kim[b], Eung Soo Kim[a,*]

[a]Department of Materials Engineering, Kyonggi University, Suwon 443-760, Korea
[b]Korea Institute of Ceramic Engineering and Technology, Seoul 153-023, Korea

Available online 23 October 2012

Abstract

The dependence of electrical properties of $[Ag_{0.2}(K_{0.52}Na_{0.48})_{0.8}](Nb_{1-x}Ta_x)O_3$ (AKNNT, $0.025 \le x \le 0.1$) ceramics on their structural characteristics was investigated. Sintered specimens had a single phase of perovskite structure with orthorhombic symmetry. The unit-cell volume and B-site bond valence (V_B) of ABO_3 perovskite structure decreased with Ta^{5+} content. This decrease induced distortion in the oxygen octahedra. The electromechanical coupling factor (k_p) and the piezoelectric constant (d_{33}) of the sintered specimens increased with octahedral distortion. Also, the dielectric constant (ε_r) increased due to the decrease in B-site bond valence (V_B). Effects of Ta^{5+} content on the remanant polarization (P_r) and coercive field (E_c) as well as mechanical quality factor (Q_m) of the sintered specimens were also discussed.

Keywords: A. Sintering; C. Electrical properties; D. Perovskites

1. Introduction

Many studies have been investigated to improve the electrical properties and sintering process of KNN-based ceramics for lead-free piezoelectric ceramics. It is well known that the ion substitution with different ionic size and electronegativity for A or B-site ion in the ABO_3 perovskite structure and generating compositions close to morphotropic phase boundary (MPB) were the effective ways to improve the electrical properties of the KNN-based ceramics [1]. However, Ag^+ substituted KNN-based ceramics such as KNN–$AgNbO_3$ [2], KNN–$AgSbO_3$ [3], KNN–$AgTaO_3$ [4] have good piezoelectrical properties (d_{33}=216 pC/N) even though compositions of ceramics did not close to the MPB. KNN–Ag based ceramics commonly formed single phase of perovskite structure with orthorhombic symmetry and the improved electrical properties of KNN–Ag based ceramics were only explained by effects of dense microstructure, ion substitution and distorted structure [2–4]. However, the relationships between structural characteristics with substitution ions and electrical properties of KNN–Ag based ceramics have been still unclear. The electrical properties of KNN based ceramics are strongly affected by structural characteristics such as displacement of octahedral cations and distortion of oxygen octahedra [1]. Therefore, the dependence of electrical properties on the structural characteristics should be studied to control and improve the electrical properties of KNN–Ag based ceramics effectively.

In this study, the electrical properties of $[Ag_{0.2}(K_{0.52}Na_{0.48})_{0.8}](Nb_{1-x}Ta_x)O_3$ (AKNNT, $0.025 \le x \le 0.1$) ceramics were investigated, as a function of Ta^{5+} content at optimum sintering conditions. The effects of structural characteristics on the electrical properties were also discussed on the basis of crystallographic considerations of oxygen octahedra and bond valence.

2. Experimental procedures

AKNNT ceramics were prepared by a conventional solid-state reaction from oxide powders with purities above 99%. Mixed powders with the desired composition were calcined at 1000 °C for 5 h, milled with 0.5 wt% MnO_2 (as an additive) and ZrO_2 balls for 24 h in ethanol, dried, and pressed isostatically at 1500 kg/cm^2 to form pellets with a diameter of 15 mm. These pellets were sintered at 1050 °C for 5 h in air based on the preliminary result for optimum density of each composition.

*Corresponding author. Tel.: +82 31 249 9764; fax: +82 31 244 6300.
E-mail address: eskim@kyonggi.ac.kr (E.S. Kim).

0272-8842/$ - see front matter © 2012 Elsevier Ltd and Techna Group S.r.l. All rights reserved.
http://dx.doi.org/10.1016/j.ceramint.2012.10.198

The apparent densities of the sintered specimens were measured using Archimedes' method. The relative densities were obtained from theoretical values. The polished surfaces of the sintered specimens were observed using a scanning electron microscope (SEM, JSM-6500 F, JEOL, Japan). Powder X-ray diffraction (XRD, D/Max-3C, Rigaku, Japan) analysis was used for the phase identification. The lattice parameters, unit-cell volumes, and atomic positions were obtained from Rietveld refinement of XRD patterns using the Fullprof program [5]. The initial structural model for KNN compounds was taken from previous reports [6]. The zero shift, individual scale factor, unit-cell parameters, and phase profile parameters (U, V, and W) along with symmetry (orthorhombic) parameter were refined until the apparent convergence of XRD patterns was reached.

Silver electrodes were formed on both surfaces of each sintered pellet by firing them at 700 °C for 10 min. The samples were polarized in a silicon oil bath at 80 °C by applying a DC electric field at 3–4 kV/mm for 20 min. The piezoelectric constant (d_{33}) was measured using a piezo-d_{33} meter (ZJ-3BN, Institute of Acoustics, Chinese Academy of Sciences, China). The electromechanical coupling coefficient (k_p), dielectric constant (ε_r), and mechanical quality factor (Q_m) were determined using the resonance and antiresonance method according to IEEE standards using an impedance analyser (HP 4192 A, Palo Alto, CA, USA).

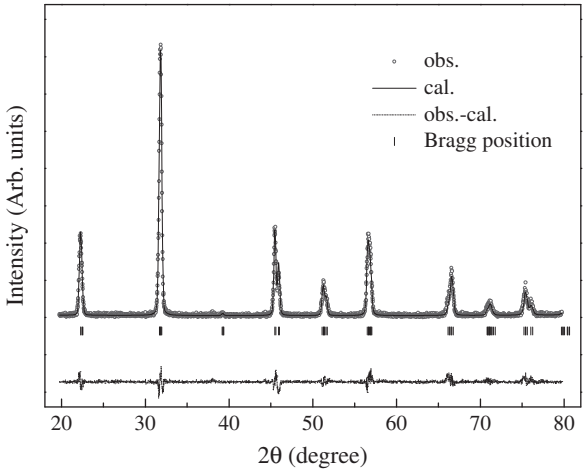

Fig. 1. Rietveld refinement patterns of $[Ag_{0.2}(K_{0.52}Na_{0.48})_{0.8}](Nb_{1-x}Ta_x)O_3$ ($x=0.1$) specimens sintered at 1050 °C for 5 h.

3. Results and discussion

3.1. Structural characteristics

Fig. 1 shows the Rietveld refinement of XRD patterns of the AKNNT ($x=0.1$) specimens sintered at 1050 °C for 5 h. A single phase of perovskite structure with orthorhombic symmetry (*Amm*2) was confirmed by the Rietveld refinement of XRD patterns for the entire compositions. Using the initial structure mode of the orthorhombic phase (ICSD ♯18502), the four types of bond lengths ($2\times d_1$, $2\times d_2$, d_3 and d_4) for the oxygen octahedra and unit-cell volumes of the sintered specimens were determined from the Rietveld refinement (Table 1). Although the ionic radius of Nb^{5+} (0.64 Å) is equal to that of Ta^{5+} for the same coordination number of 6 [7], the unit-cell volume decreased with increasing Ta^{5+} content. These results were related to octahedral distortion. The distortion of NbO_6 octahedra was calculated using equation [8]

$$\Delta = \frac{1}{6}\sum\left\{\frac{R_i-\overline{R}}{\overline{R}}\right\}^2 \quad (1)$$

where R_i is the individual bond length and $\overline{R}$ is the average bond length of the oxygen octahedra. With increase of Ta^{5+} content, the value of octahedral distortion increased. This result indicated that displacement of B-site ion was enhanced by Ta^{5+} substitution due to the higher polariziability of Ta^{5+} (4.73 $Å^3$) than Nb^{5+} (3.97 $Å^3$). The distortion tends to be larger if the ions involved have higher polariziability [9]. Also, hybridization of covalency bonding between one oxygen and Ta^{5+} ion could be reason for induced octahedral distortion [1].

The polariziaibilty difference of Ta^{5+} from Nb^{5+} also affected the bond length and bond strength of the composing ions of AKNNT ceramics. The bond length and bond strength between B-site ion and oxygen could be evaluated by bond valence. The bond valences (V_B) between B-site cations and oxygen ions in ABO_3 perovskite structure were calculated using equations [10]

$$V_B = \sum_{j=1}^{N} v_{B-O} \quad (2)$$

$$v_{B-O} = \exp[(R_{B-O}-d_{B-O})/b] \quad (3)$$

Table 1
Relative density and structural characteristics and mechanical quality factor (Q_m) for $[Ag_{0.2}(K_{0.52}Na_{0.48})_{0.8}](Nb_{1-x}Ta_x)O_3$ specimens sintered at 1050 °C for 5 h.

x (mole)	Relative density (%)	B-site bond length (Å)				Unit-cell volume (Å^3)	V_B	Octahedral distortion ($\Delta\times10^4$)	R_{Bragg}	Gof	Q_m
		d_1	d_2	d_3	d_4						
0.025	92.876	2.055	1.949	1.976	2.031	125.827	4.88	17.359	7.39	2.7	175.37
0.05	93.062	1.878	2.116	1.972	2.049	125.747	4.77	24.895	6.29	2.5	174.17
0.075	93.448	1.859	2.147	1.982	2.054	125.536	4.71	35.629	5.93	2.2	172.16
0.1	93.735	1.849	2.167	1.983	2.060	125.337	4.66	42.934	7.31	2.2	157.64

V_B is B-site bond valence, R_{Bragg} is Bragg R-factor and Gof is goodness of fit.

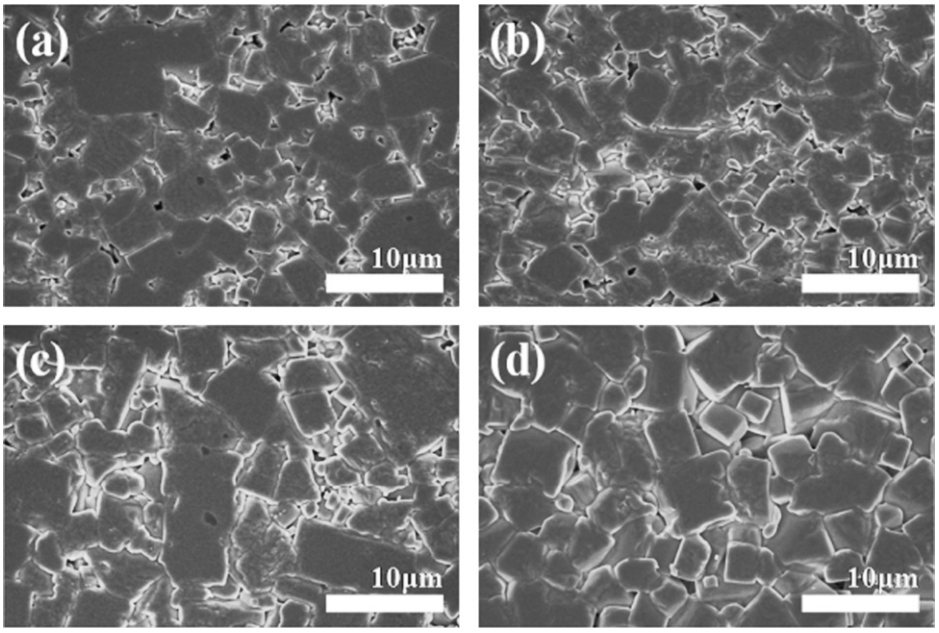

Fig. 2. SEM micrographs of $[Ag_{0.2}(K_{0.52}Na_{0.48})_{0.8}](Nb_{1-x}Ta_x)O_3$ ($0.025 \le x \le 0.1$) specimens sintered at 1050 °C for 5 h; (a) $x=0.025$, (b) $x=0.05$, (c) $x=0.075$, and (d) $x=0.1$ (bar = 10 μm).

where R_{B-O} is the bond valence parameter, d_{B-O} is the bond length between B-site cations and oxygen ions, and b is generally taken to be a universal constant equal to 0.37 Å [11]. The values for the bond valence parameters matched in Brese's report [10]. The bond lengths were calculated using the Rietveld method (Table 1). The V_B decreased with Ta^{5+} content, which could affect the dielectric constant (ε_r) of the ceramics.

AKNNT specimens ($0.025 \le x \le 0.1$) that were sintered at 1050 °C for 5 h showed relative densities of above 93% (Table 1). SEM micrographs of the AKNNT specimens sintered at 1050 °C for 5 h are shown in Fig. 2. The ceramics with $x=0.025$ had inhomogeneous and the abnormal grains were observed. For the ceramics with $x=0.1$, a rectangular morphology and dense microstructure was observed, which agrees with the results of relative density (Table 1). With increasing of Ta^{5+} content, orthorhomic-tetragonal phase transition temperature (T_{o-t}) shifted toward the lower-temperature regions and the octahedral distortion increased.

3.2. Electrical properties

Fig. 3 shows the *P–E* hysteresis loops of the AKNNT specimens sintered at 1050 °C for 5 h. With increasing Ta^{5+} content, the remanant polarization (P_r) of the specimen increased, while the coercive field (E_c) decreased. The ceramics with $x=0.1$ possess a large remanant polarization ($P_r = 22.4\ \mu C/cm^2$) and small coercive field ($E_c = 0.5$ kV/mm). The spontaneous polarization (P_s) increased and E_c decreased with Ta^{5+} content. These result could be explained by following equation [12]:

$$P_s \sim K(\Delta z_{eff}) \quad (4)$$

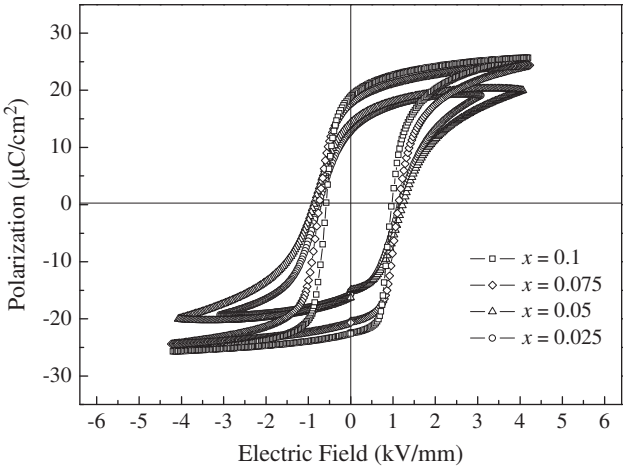

Fig. 3. *P–E* hysteresis loops of $[Ag_{0.2}(K_{0.52}Na_{0.48})_{0.8}](Nb_{1-x}Ta_x)O_3$ ($0.025 \le x \le 0.1$) specimens sintered at 1050 °C for 5 h.

where $K = (258 \pm 9)\ \mu C cm^{-2}$ Å, Δz_{eff} is the ionic effective displacement of the active ferroelectric ion, P_s is spontaneous polarization.

This equation indicated that high value of displacement of the B-site central ion from its equilibrium position induced spontaneous polarization and remanant polarization. Similarly, octahedral distortion increased with substitution of Ta^{5+} content (Table 1), which induced remanant poalrization for AKNNT ceramics (Fig. 3).

On the other hand, the high polarization is directly proportional to piezoelectric constant (d_{33}). Marcos et al. suggested the following equation [13]:

$$d_{33} = 2Q_{11}P_s\varepsilon_{33} \quad (5)$$

where Q_{11} is the longitudinal transverse electrostrictive coefficients. Thus, large dielectric constants and high polarizations are required to produce a large induced piezoelectric constant. These factors could also be confirmed for AKNNT ceramics in this study.

Fig. 4 shows the dependence of the d_{33} and k_p on the octahedral distortion of the AKNNT specimens sintered at 1050 °C for 5 h. With increasing Ta^{5+} content, the octahedral distortion also increased causing d_{33} and k_p of the specimens to increase. Octahedral distortion related to displacement of B-site cation in ABO_3 perovskite structure. Therefore, induced off-centering of B-site ion increased vibration of lattice, which improved the piezoeletric properties [9].

Fig. 5 shows ε_r at 1 kHz for the AKNNT specimens sintered at 1050 °C for 5 h. With increasing Ta^{5+} content, ε_r of the specimens increased due to the decrease of V_B (Table 1) [14]. Low V_B indicated low bond strength between oxygen and B-site ion. Therefore, B-site ion was more rattling in the oxygen octahedra, which induced large dielectric constant (ε_r) of AKNNT ceramics. However, Q_m of the sintered specimens at $x=0.1$ had lower value than $x=0.025$ specimens (Table 1) even though dense microstructure was confirmed at $x=0.1$ (Fig. 1). Decrease of Q_m could be attributed to internal friction as a result of the octahedral distortion of crystal structure. With increasing Ta^{5+} content, the increased octahedral distortion improved the piezoelectric properties (d_{33}, and k_p) and ferroelectric properties (P_r, and P_s). These results imply that the domain walls are easier to move under the driving electric field, which always leads to the increase of the internal friction of the ceramics and the decrease of Q_m [15].

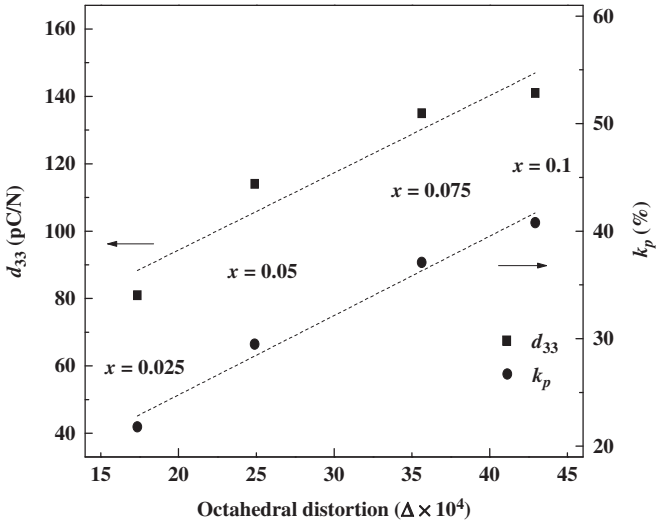

Fig. 4. Dependence of piezoelectric constant (d_{33}) and electromechanical coupling factor (k_p) on octahedral distortion (Δ) of $[Ag_{0.2}(K_{0.52}Na_{0.48})_{0.8}](Nb_{1-x}Ta_x)O_3$ ($0.025 \le x \le 0.1$) specimens sintered at 1050 °C for 5 h.

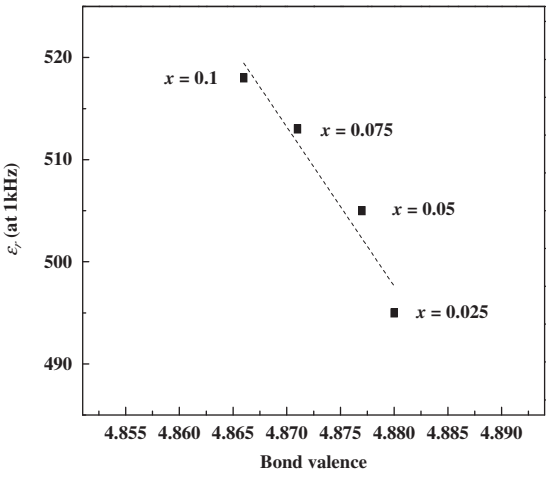

Fig. 5. Dependence of dielectric constant (ε_r) on B-site bond valence (V_B) of $[Ag_{0.2}(K_{0.52}Na_{0.48})_{0.8}](Nb_{1-x}Ta_x)O_3$ ($0.025 \le x \le 0.1$) specimens sintered at 1050 °C for 5 h.

4. Conclusions

For the AKNNT ($0.025 \le x \le 0.1$) specimens sintered at 1050 °C for 5 h, a single phase of perovskite structure with orthorhombic symmetry was detected through the entire range of compositions. The values of d_{33} and k_p of the sintered specimens increased with the Ta^{5+} content. These results could be affected by the octahedral distortion. Also, octahedral distortion enhanced the ferroelectricity of the sintered specimens. ε_r of the sintered specimens increased because of the decrease in B-site bond valence (V_B) of ABO_3 perovskite structure. However, Q_m of the sintered specimens decreased due to increase of internal friction by octahedral distortion.

Acknowledgements

This research was supported by a grant from the Fundamental R&D Program for Core Technology of Materials funded by the Ministry of Knowledge Economy, Republic of Korea.

References

[1] Y. Saito, H. Takao, Lead-free piezoceramics, Nature 432 (2004) 84–87.
[2] C. Lei, Z.Guang Ye, Lead-free piezoelectric ceramics derived from the $K_{0.5}Na_{0.5}NbO_3$–$AgNbO_3$ solid solution system, Journal of Applied Physics Letters 93 (2008) 042901–042903.
[3] Y. Wang, Q. Liu, J. Wu, Piezoelectric properties of $(1-x)(Na_{0.5}K_{0.5})NbO_3-xAgSbO_3$ lead-free ceramics, Journal of the American Ceramic Society 92 (2009) 755–757.
[4] Y. Wang, L. Qibin, F. Zhao, Phase transition behavior and electrical properties of $[(K_{0.5}Na_{0.5})_{1-x}Ag_x](Nb_{1-x}Ta_x)O_3$ lead-free ceramics, Journal of Alloys and Compounds 489 (2010) 175–178.
[5] T. Roisnel, J.R. Carvajal, WinPLOTR: a windows tool for powder diffraction patterns analysis, Materials Science Forum 378–381 (2001) 118–123.
[6] V.A. Shuvaeva, M.Y. Antipin, Structural disorder in $KNbO_3$ crystal from X-ray diffraction and EXAFS spectroscopy, Kristallografiya 40 (1995) 511–516.
[7] M. Suewattana, Local dynamic and structure of pure and Ta substituted $(K_{1-x}Na_x)NbO_3$ from first principles calculations, Physical Review B 82 (2010) 014114–014115.

[8] R.D. Shannon, Effective ionic radii in oxides and fluorides, Acta Crystallographica Section B 25 (1969) 925–946.
[9] A. Khalal, D. Khatib, Elastic and piezoelectric properties of $PbTiO_3$ at room temperature, Ferroelectrics Letters Section 26 (3-4) (1999) 91–98.
[10] N.E. Brese, M. O'Keeffe, Bond-valence parameters for solids, Acta Crystallographica Section B 47 (1991) 192–197.
[11] I.D. Brown, D. Altermatt, Bond-valence parameters obtained from a systematic analysis of the inorganic crystal structure database, Acta Crystallographica Section B 41 (1985) 244–247.
[12] S.C. Abrahams, Atomic displacement relationship to curie temperature and spontaneous polarization in displacive ferroelectrics, Physical Review 172 (1968) 551–553.
[13] F. Rubio-Marcos, M.A. Banares, Correlation between the piezoelectric properties and the structure of lead-free KNN-modified ceramics, studied by Raman spectroscopy, Journal of Raman Spectroscopy 42 (2011) 639–643.
[14] E.S. Kim, B.S. Chun, D.H. kang, Effects of structural characteristics on microwave dielectric properties of $(1-x)Ca_{0.85}Nd_{0.1}TiO_3-xLnAlO_3$ (Ln=Sm, Er and Dy) ceramics, Journal of the European Ceramic Society 27 (2007) 3005–3010.
[15] Y. Cheng, Y. Yang, Y. Wang, H. Meng, Study on $Pb(Mg_{1/3}Ta_{2/3})$-O_3–$Pb(Mn_{1/3}Sb_{2/3})O_3$–$Pb(ZrxTi_{1-x})O_3$high power piezoelectric ceramics near the morphotropic phase boundary, Journal of Alloys and Compounds 508 (2010) 364–369.